Transient nuclear envelope rupturing during interphase in human cancer cells

Jesse D. Vargas, Emily M. Hatch, Daniel J. Anderson and Martin W. Hetzer*

Molecular and Cell Biology Laboratory; Salk Institute for Biological Studies; La Jolla, CA USA

Neoplastic cells are often characterized by specific morphological abnormalities of the nuclear envelope (NE), which have been used for cancer diagnosis for more than a century. The NE is a double phospholipid bilayer that encapsulates the nuclear genome, regulates all nuclear trafficking of RNAs and proteins and prevents the passive diffusion of macromolecules between the nucleoplasm and the cytoplasm. Whether there is a consequence to the proper functioning of the cell and loss of structural integrity of the nucleus remains unclear. Using live cell imaging, we characterize a phenomenon wherein nuclei of several proliferating human cancer cell lines become temporarily ruptured during interphase. Strikingly, NE rupturing was associated with the mislocalization of nucleoplasmic and cytoplasmic proteins and, in the most extreme cases, the entrapment of cytoplasmic organelles in the nuclear interior. In addition, we observed the formation of micronuclei-like structures during interphase and the movement of chromatin out of the nuclear space. The frequency of these NE rupturing events was higher in cells in which the nuclear lamina, a network of intermediate filaments providing mechanical support to the NE, was not properly formed. Our data uncover the existence of a NE instability that has the potential to change the genomic landscape of cancer cells.

Introduction

The nuclear envelope (NE) is a physical membrane barrier that separates the nucleus from the cytoplasm. It fulfills at least two essential functions in eukaryotic cells: first it regulates the movement of molecules between the nucleus and the cytoplasm by active, signal-dependent transport via aqueous channels that are formed by the nuclear pore complexes (NPCs), and second it creates a permeability barrier that prevents the passive diffusion of molecules larger than ~40 kDa across the NE. An intact nuclear permeability barrier is generally considered to be a prerequisite for nuclear transport and to be critical for proper cell compartmentalization.

Morphologically and structurally abnormal nuclei are frequently observed in cancer cells.[1] Morphometric criteria such as NE invaginations, extrusions and lobes are routinely used in the clinic for cancer diagnostics and prognosis,[2] and in some cases, karyometric features were found to be more appropriate than biomarkers to predict metastases.[3] Despite the clinical relevance of aberrant NE morphology, it remains unclear why such changes to the NE are more prevalent in cancer cells, and if these characteristic morphological features of the NE contribute to cell transformation and tumor formation.

The nuclear lamina is an intermediate filament network comprised of lamin proteins that assembles on the inner nuclear membrane (INM). It is connected to the NE via interactions with INM proteins and provides structural support, mechanical stiffness and elasticity to the nuclear membrane. Two major types of lamin are present in human somatic cells: the A-type lamins include lamin A and lamin C, which are different isoforms of a single gene, and the B-type lamins that include lamin B1 and lamin B2, which are encoded by separate genes. Both types of lamins are important for stabilizing the nuclear membrane,[4-7] and, along with various interacting proteins, are thought to organize the nucleus by localizing specific proteins responsible for chromatin organization, cell cycle control, and transcription regulation to the nuclear periphery.[8] Lamin B1 is important for development; mice homozygous for non-functional lamin B1 die at birth.[9] In addition, mutations in the lamin genes that alter lamin protein expression and disrupt the formation of the lamina cause a group of pleiotropic developmental diseases called laminopathies.[10] These disorders are characterized by changes in the mechanical properties of the nucleus[4,11-13] and affect mainly cells under mechanical stress.[14]

The NE is a dynamic structure that undergoes complete disassembly and reformation during the cell cycle. Nuclear

envelope breakdown (NEBD) occurs only at the onset of mitosis and facilitates the equal segregation of the genome and other cellular components into two daughter cells. NEBD is initiated by a series of phosphorylation events that trigger the breakdown of the NPCs and lamina and is followed by the retraction of the NE into the mitotic endoplasmic reticulum (ER).[15-17] NE re-formation during late anaphase/telophase is a rapid process that involves distinct groups of INM proteins with redundant functions driving a rapid and massive reorganization of the ER to surround the decondensing chromatin.[18-21]

Given the functional importance of an intact NE, it was generally assumed that mixing of the cytoplasmic and nuclear compartments occurs only during mitosis. However, a recent study reported a temporary loss of cell compartmentalization by NE rupturing during interphase in cells isolated from laminopathy patients.[22] Since changes in NE structure are an early diagnostic criteria of malignant cell growth[2] and many cancer cells have decreased expression of lamins or other structural nuclear proteins both in tumors[23-30] and in culture,[28,31,32] we wondered whether nuclear membrane integrity is compromised in cancer cells. Additionally, we were curious what might be the physiological consequences if lapses in interphase nuclear integrity occurs in cancer. Here we demonstrate that transient NE rupturing during interphase (NERDI), an event that involves an interphase loss of the nuclear permeability barrier and mixing of normally separated nuclear and cytoplasmic components, occurs in several commonly used human cancer cell lines. Further, we show that such ruptures result in significant mislocalization of nuclear and cytoplasmic factors. Our results suggest that this phenomenon may stimulate several fundamental processes associated with tumorigenesis like misregulation of growth signaling pathways and increased genomic instability.

Results

Transient mislocalization of nuclear GFP$_3$-NLS in cancer cells. To study potential defects in NE integrity in cancer cells, we used GFP$_3$-NLS (three copies of GFP fused to the nuclear localization signal of the SV40 large T antigen) as a live-cell nuclear integrity reporter. Nuclear accumulation of this ~80 kD reporter occurs during interphase and requires both active nuclear import and the presence of an intact NE.[18,20,33] Localization of this reporter to the cytoplasm is indicative of NEBD, which occurs during early prophase (**Fig. S1A** NE in green, open arrows and **Fig. S1B**, open arrows) as the NE is retracted into the mitotic ER, and its re-localization to the nucleus in late anaphase/early telophase

corresponds to NE reformation (**Fig. S1A** NE in green, solid arrows and **Fig. S1B**, solid arrows) and the resumption of active nuclear transport (**Fig. S1A and B**).[15,16,18,20,33] To test whether non-mitotic NE rupturing can also be visualized using this reporter, we transfected a human U2OS osteosarcoma cell line expressing GFP$_3$-NLS with a FLAG tagged version of the HIV-1 protein Vpr, which has been shown to rupture the NE during interphase leading to cell cycle arrest in G$_2$.[34] In contrast to control cells, GFP$_3$-NLS was mislocalized to the cytoplasm in cells expressing Vpr-FLAG (**Fig. S1C**, arrows). Consistent with a previous report, Vpr-induced NE rupturing was extensive with nuclear ruptures persisting for several hours without repair (**Fig. S1D**).[34]

Having established a reliable assay to monitor NE integrity throughout the cell cycle, we transfected and monitored the localization of GFP$_3$-NLS in U2OS cells over a period of at least 36 h. Images were acquired with a 3 min time interval to ensure that NE integrity was observed with sufficient temporal resolution throughout the cell cycle. We observed that in a rare subset of U2OS cells (~8% of cells in a population) GFP$_3$-NLS transiently appeared in the cytoplasm concomitant with a decrease in nuclear signal and in the absence of mitotic division (**Fig. 1A**, **Vid. S1**). Remarkably, the temporary efflux of GFP$_3$-NLS out of the nucleus was followed by the proper re-accumulation of the reporter into the nucleus and these events could be observed to occur several times within individual cells (**Fig. 1A**, arrows). To determine the kinetics of interphase NE ruptures we measured the fluorescence intensity of the GFP$_3$-NLS in the nucleoplasm and cytoplasm over the course of this event. The loss of nuclear integrity was extremely rapid with virtually complete equilibration of nuclear and cytoplasmic GFP intensity occurring within a single frame (< 3min) (**Vid. S1**). This was followed by a slower recovery period on a timescale similar to that of post-mitotic NE reformation.[18,20]

In order to examine the dynamics of individual spilling events we employed curve fitting algorithms to interphase NE rupture events imaged with high (30 sec) temporal resolution. To calculate the rate of recovery after NERDI events, we measured the nuclear and cytoplasmic intensity of GFP-NLS and fit these intensities to a segmented regression where the intact nuclei were fit to a plateau constant, spilling events were fit to a linear regression and recovery events were fit to a sigmoidal curve (mean R^2 = 0.97) (**Fig. 1B**). We hypothesize that recovery after NERDI fits well to a sigmoidal curve rather than an exponential curve because nuclear import likely begins before ruptures are fully closed. This analysis gave recovery half-times of ~6 min

Figure 1 (See next page). Nuclear envelope rupture during interphase. (A) U2OS cells transiently transfected with GFP$_3$-NLS and imaged every 3 min for 36 h show transient interphase rupturing of the NE followed by recovery of GFP$_3$-NLS into the nucleus. (B) Dynamics of a rupture event. U2OS cells expressing GFP-NLS were imaged every 30s to capture NERDI in high temporal resolution. GFP intensity was normalized by setting the maximum and minimum intensity for each cell to 1 and 0, respectively. Curve fittings of individual interphase NE ruptures were plotted (lines) along with raw data (points). Data was fit using the equation: $Y = IF(X < X0, Y0, IF(X < X1, Y0-S*X, Bottom+(Top-Bottom)/[1+10^{((Log50-X)*HillSlope)}]))$ where: X0 is the point of inflection between the plateau and the spilling event, Y0 is the plateau value, X1 is the initial point of recovery, S is the slope of spilling, Bottom is the lower plateau for recovery, Top is the upper plateau of recovery, Log50 is the point of 50% recovery, and HillSlope is the linear rate of recovery. (C) Representative images of HeLa cervical and SJSA osteosarcoma cancer cell lines demonstrating spilling in diverse cancer cell types. (D) U2OS cells transiently transfected with GFP$_3$-NLS and imaged every 3 min show localized nuclear deformation and cytoplasmic GFP signal originating from the site of deformation.

although some cells seemed to struggle to repair the NE taking up to 9 min to reach the same 50% fluorescence recovery point (**Fig. 1B**).

It is important to note that the frequency of NE rupturing during interphase (NERDI) did not increase with laser excitation intensity, exposure time, or expression level of the GFP_3-NLS
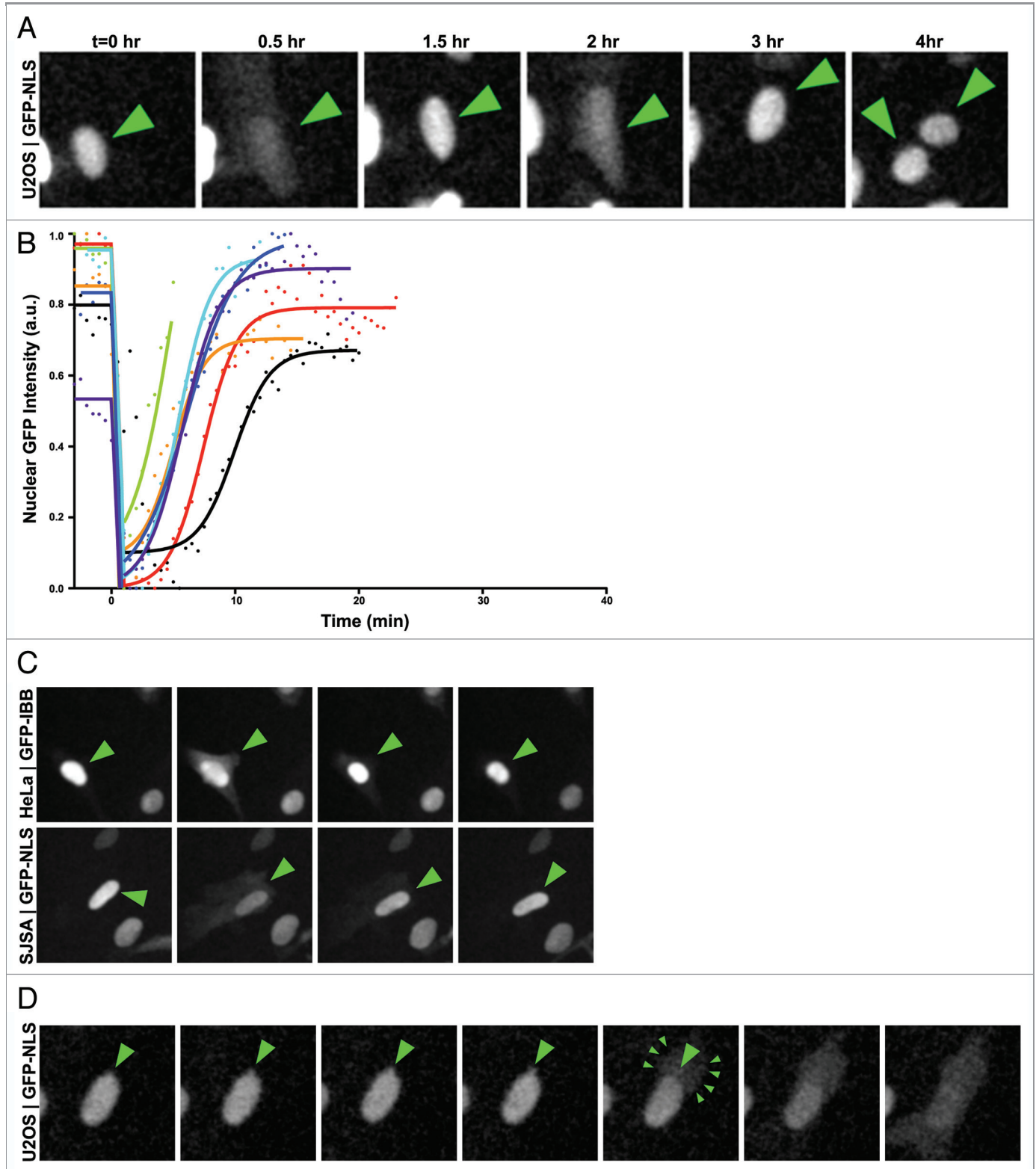
reporter (data not shown). Thus, it is unlikely that interphase loss of NE integrity is a result of experimental design or imaging. In addition, the disruption of the NE barrier did not result in apoptosis, as indicated by the ability of the cells to re-accumulate their nuclear contents, persist in culture, and go on to complete cell division and cytokinesis (**Fig. 1A**, right panels; **Vids. S2 and S3**).

To determine whether NERDI is specific to U2OS cells, we expressed and observed the dynamics of a nuclear reporter in two additional cancer cell lines, the human HeLa (cervical carcinoma) and SJSA (osteosarcoma) cell lines. We observed transient mislocalization of the reporter to the cytoplasm during interphase in both of these cell lines (**Fig. 1C**), indicating that NERDI is not specific to U2OS cells and affects cancer cell lines arising from divergent tissues. Importantly as a control, in primary human fibroblast IMR90 cells we observed less than 1% of cells exhibiting interphase NE rupture (**Fig. 2A**). Our results from the single primary cell line are limited but suggest that NERDI may be more common in malignant cells and could correlate with the well-described alterations in NE structure in cancer cells.

Analyzing still images of NERDI in U2OS cells revealed that nuclear ruptures initiate from localized deformations of the NE (**Fig. 1D**, large arrows; **Vid. S4**). These NE herniations expand and eventually rupture, with the observed efflux of GFP$_3$-NLS appearing initially in the cytoplasmic region proximal to the site of NE herniation before rapidly diffusing throughout the cell body (**Fig. 1D**, small arrows; **Vid. S4**). This observation suggests that interphase losses in nuclear integrity originate from large structural changes in the NE.

Knockdown of lamins increases the frequency of NE rupturing during interphase. Since aberrations in the nuclear lamina have been shown to affect the mechanical properties of the NE,[35,36] and since the NE herniations observed prior to rupturing are reminiscent of structures seen in cells lacking either lamin B1 or lamins A and C,[9,11] we reasoned that altered lamin organization might be facilitating interphase nuclear rupturing in U2OS cells. To test this idea, we treated U2OS cells with either a scrambled siRNA or a cocktail of siRNAs directed against the three nuclear lamin genes, lamin A/C, B1, and B2, that effectively targets each of the three lamins in individual cells (**Fig. S2A**). We found that transfection efficiency limited the population-averaged reduction in lamin protein levels to ~20% by protein gel blot (**Fig. S2B**),

and that this reduction led to a statistically significant ($p < 0.05$) increase in the frequency of nuclear rupture events compared with control siRNA (**Fig. 2A**). In contrast, cells knocked down for the NPC components Nup93 or Nup107, or the INM proteins LBR and Lap2β in combination, had no statistically significant increase in NERDI frequency ($p = 0.21$, 0.34, and 0.45 respectively) (**Fig. 2A**). These results further support our model that NERDI is not due to changes in the passive diffusion limit, but rather to large-scale disruptions of the nucleus. Nuclear pore defects as a contributing factor to NERDI are made further unlikely by the rapid and mass movement of GFP$_3$-NLS into the cytoplasm, which suggests a large temporary tear in the NE rather than a continual pore-associated leakiness.

Additional evidence for lamins normally functioning to prevent NERDI came from results from transmission electron microscopy (TEM) performed on U2OS cells stably expressing an shRNA against lamin B1 that resulted in a similar frequency (~25%) of NERDI as the triple siRNA cocktail. In lamin B1 shRNA cells stained with tannic acid to enhance the nuclear lamina (**Fig. 2B**, solid arrows) nuclear herniations similar to those seen in live-imaging just prior to NE rupture are clearly visible (**Fig. 2B**, enlargements). Of note, areas where the NE is distended have a marked absence of electron density (**Fig. 2B**, open arrows), suggesting that these areas, which are prone to rupture, are deficient in lamin assembly. The interior of the NE herniations often exhibit a gradation in staining by TEM with darker nucleoplasm-like material near the nuclear interior blending with lighter cytoplasmic-like material in the distal area of the herniation (**Fig. 2B**), as would be expected if the nuclear and cytoplasmic compartments had previously mixed at this location.

In addition to the increased NERDI frequency, the recovery time of cells treated with the triple lamin knock-down significantly increased ($p < 0.05$) from an average of ~6 min for control cells to ~12 min for 3 lamin siRNA (**Fig. 2C and D**), indicating that lamins both prevent nuclear rupturing and promote the repair of NE rupturing. The ability of lamin reduction to increase the frequency of NERDI, as well as to increase the time required to recover from such defects further supports the idea that the observed phenomenon is a consequence of altered nuclear structure.

Our observations that NERDI increases with reduced lamin expression are particularly interesting since reduced and aberrant

Figure 2 (See next page). Reduced lamin levels accentuate nuclear ruptures. (A) Frequency of NERDI in U2OS cells after treatment with two rounds of knock down by siRNA directed against: the three lamin genes, LBR and Lap2b, Nup93, or Nup107, compared with reporter only (none), scrambled siRNA, or non-transfected IMR90 controls (p = 0.02 3LamKD vs Scram. siRNA). Cells were imaged for a period of 36 h and frequencies represent the proportion of cells that experience an interphase NE rupture at least once over the course of the experiment. (B) Transmission electron microscopy (TEM) of U2OS stably reduced for lamin B1 expression by shRNA and stained with tannic acid to enhance lamin visualization (solid arrows). Characteristic NE herniations exhibit reduced tannic acid staining (open arrows). (C) Dynamics of a rupture in U2OS cells treated with 3 lamin siRNA. U2OS cells transfected with GFP-NLS and three lamin siRNA pool were imaged every 30s to capture NERDI in high temporal resolution. Curve fittings, as in **Figure 1B**, of individual interphase NE ruptures are plotted (lines) along with raw data (points) and show the dynamics of the event. (D) Recovery half-lives of rupture were obtained from each curve and averaged for control and three lamin siRNA treated cells with measured half-lives of ~6 and ~12 min, respectively. (E) Left: U2OS cells stably reduced for lamin B1 expression by shRNA and expressing the GFP$_3$-NLS reporter were transiently transfected with either mCherry alone or human lamin B2 tagged with mCherry (mCherry-LmnB2). Frequency of NERDI was analyzed in transfected cells imaged for 36 h. Cells with mCherry-LmnB2 aggregates were excluded from analysis. Right: Average number of spills per cell was determined for cells transfected with either mCherry or mCherry-LmnB2 and imaged for 36 h. For both, n ≥ 340 cells over two experiments. Error bars are standard error and the difference in percent cells with spilling nuclei is significant (p ≤ 0.01) by Student's t-test.
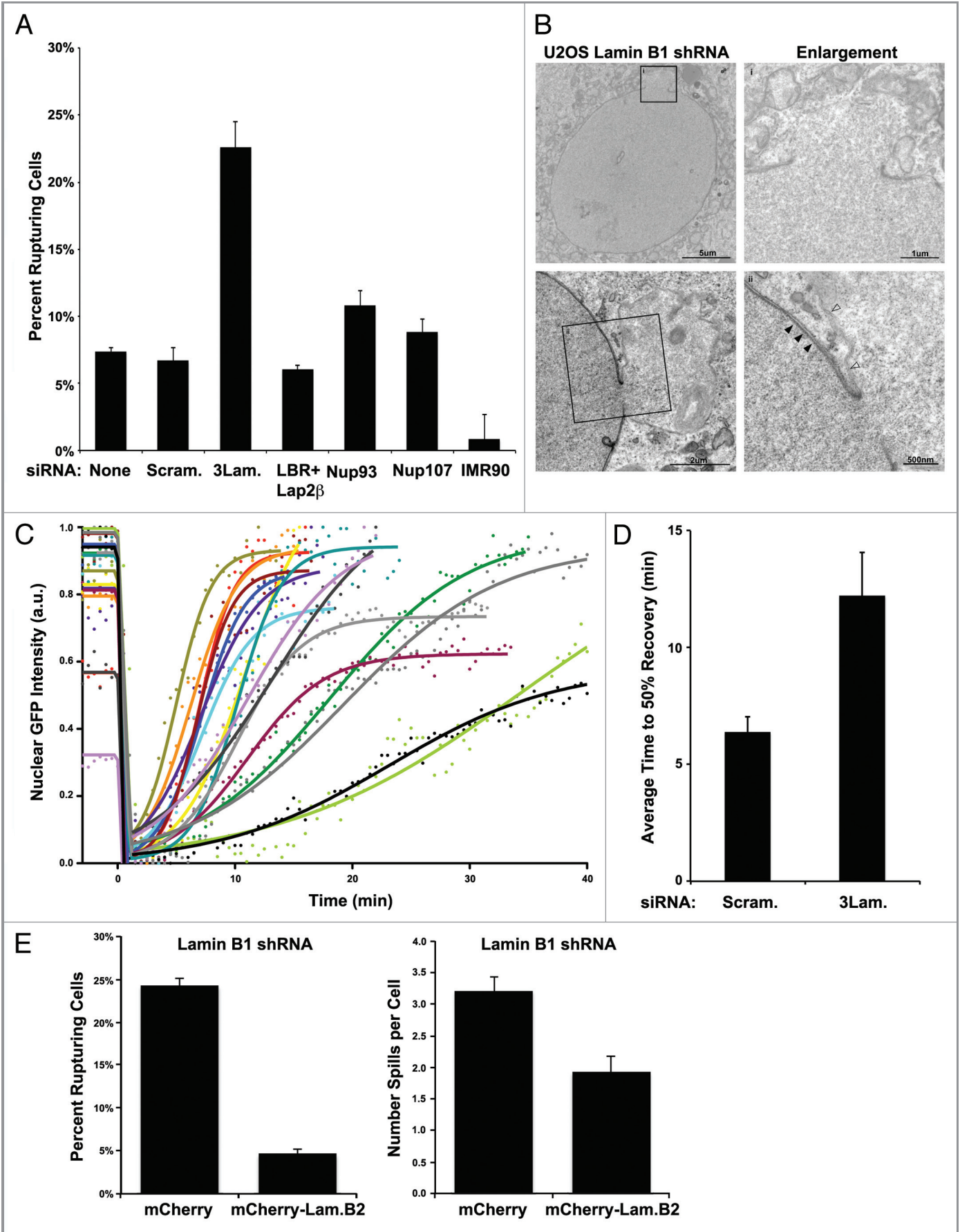
expression of nuclear lamins has previously been reported in tumor tissue.[23-30] Interestingly, we found that lamin levels were not uniform in U2OS cells; immunofluorescence using antibodies against lamin B1 and B2 revealed significant differences in lamin staining within a single field of cells (**Fig. S2C**). This variation, which is also present in various cell cycle phases of U2OS cells synchronized by double thymidine block (data not shown), could underlie the differences in spilling frequency we observe in normal U2OS cells. Likewise, consistent with other reports,[28,31,32] we found that lamin protein levels also vary widely between different cancer cell lines as determined by protein gel blot (**Fig. S2D**). Of note, several breast cancer lines exhibited lower levels of lamin expression, including those classified as particularly invasive, compared with the non-transformed MCF-10A line that retains breast tissue specific differentiation characteristics (**Fig. S2D**). The lines with the most reduced lamin levels were not conducive to our live-imaging approach and so the presence of interphase nuclear rupturing in them remains uncertain.

Because depletion of lamins has been shown to have diverse effects on nuclear organization and functions,[37,38] we wanted to ensure the phenotype we observed was the result of changes in NE structure and not downstream effects on gene expression or chromatin reorganization. To do this, we overexpressed the other B-type lamin, lamin B2, in U2OS cells depleted of lamin B1 and observed NERDI frequency. Depletion of lamin B1 alone by shRNA gave a robust knock down of lamin B1 in individual cells (**Fig. S3A**) and an overall reduction in lamin B1 levels by protein gel blot (**Fig. S3B**). Lamin B2 functions similarly to lamin B1 in structuring the NE,[37,39] and our expression construct localized as expected in control U2OS cells and without disrupting endogenous lamin B1 (**Fig. S2E**). While lamin B2 localizes to the NE similar to lamin B1, it is unlikely to have the same protein interactions, as lamin B2 null mice have distinct phenotypes.[40] We reasoned that expression of lamin B2 might compensate for the structural deficits of the lamin B1 depletion. To test this, U2OS cells stably depleted of lamin B1 were transfected with either mCherry-lamin B2 or mCherry alone. Expression of mCherry-lamin B2 was able to significantly decrease (p = 0.005) the percentage of cells exhibiting NERDI, as well as decrease the average number of times each rupturing cell ruptured (**Fig. 2E**), suggesting that it is the structural function of the lamins that normally maintains interphase nuclear integrity, and not their functions in interphase nuclear organization or transcription.

Interphase NE rupturing causes mislocalization of cellular components. Having established that our GFP-reporter is mislocalized to the cytoplasm during transient NE rupturing, we next wondered whether endogenous nucleoplasmic proteins would also be present in the cytoplasm during NE rupturing. Since our reporter for nuclear integrity is a soluble protein, we postulated that other soluble nuclear factors might be released into the cytoplasm during an interphase rupture event. We first characterized the localization of eIF4AIII, a member of the DEAD-box family of RNA helicases and a soluble nuclear factor that is part of the exon junction complex loaded onto mRNAs inside the nucleus.[41] We observed eIF4AIII localizing in the nucleus and NE herniations during interphase by immunofluorescence in U2OS cells stably expressing an shRNA against lamin B1 (**Fig. 3A**, top panels arrows). In cells with ruptured NEs, as identified by cytoplasmic GFP3-NLS localization and the absence of DNA condensation (**Fig. 3A**, bottom panels arrows), eIF4AIII was mislocalized to the cytoplasm (**Fig. 3A**), indicating that endogenous proteins are misplaced from the nucleus during NERDI. We also observed an increase in diffuse nuclear tubulin staining concomitant with NERDI (**Fig. 3A**, middle panels solid vs. open arrows, see enlarged tubulin signal enhancement on right), suggesting that the loss of the permeability barrier across the NE occurs in both directions.

In order to confirm altered localization of cytoplasmic proteins during NERDI and that loss in nuclear integrity is bidirectional, we stained fixed U2OS cells expressing the lamin B1 shRNA with antibodies against UPF1, a cytoplasmic mRNA factor that is recruited upon recognition of a stop codon by the translation machinery.[42] Immunofluorescence imaging of U2OS cells stably reduced for lamin B1 to increase the frequency of NERDI showed that UPF1 is present within the interphase nucleus when nuclei undergo interphase rupture, as evidenced by GFP3-NLS presence in the cytoplasm (**Fig. 3B**, top panels arrows). Again interphase rupture is distinguished from mitotic rupture by comparison to mitotic cells where the chromatin is clearly condensed and the mitotic spindle is visible (**Fig. 3B**, bottom panels arrows). Although both cytoplasmic and nuclear proteins, specifically those involved in mRNA processing, are mislocalized during transient rupturing, it is plausible that their aberrant localization is corrected either by nuclear import/export machinery or during the next division cycle. In all observed cases their mislocalization coincided with a loss of nuclear integrity, as determined by efflux of GFP3-NLS from the nucleus. Therefore, it is likely that NERDI associated mislocalization of protein factors is recoverable as long as such factors carry appropriate localization signals, or in the worst case scenario factors could be reapportioned during the next mitotic cycle.

Figure 3 (See next page). Mislocalization of nuclear and cytoplasmic components. (A) U2OS cells stably reduced for lamin B1 expression by shRNA, expressing GFP3-NLS reporter and stained with antibodies against eIF4AIII (red), tubulin (white), and for DNA with Hoechst (blue) show characteristic NE herniations (top arrows), and cytoplasmic localization of eIF4AIII during an interphase NE rupture (middle panel, arrows) with corresponding nuclear influx of soluble tubulin (middle, solid vs. open arrows) contrasted from mitotic NEBD with characteristic condensed DNA and tubulin spindle (bottom panel, arrows). Zoom panel shows linear brightness increase for visualization of diffuse nuclear tubulin. (B) U2OS cells treated as in part A stained for UPF1 (red) and tubulin (white). UPF1 is present in the nuclear interior during an interphase rupture event (top panel, arrows) contrasted from mitotic NEBD by chromatin structure and mitotic spindle (bottom panels, arrows). (C) Time series images of NERDI in U2OS cell showing NE deformation and rupture and chromatin dynamics during the event. Nuclear integrity was monitored with GFP3-NLS (green) and chromatin with H2B-mCherry (red) reporters. GFP3-NLS diffuses throughout cytoplasm during NE rupture; H2B-mCherry spills into cytoplasm but is contained to a localized area just beyond the NE boundary.
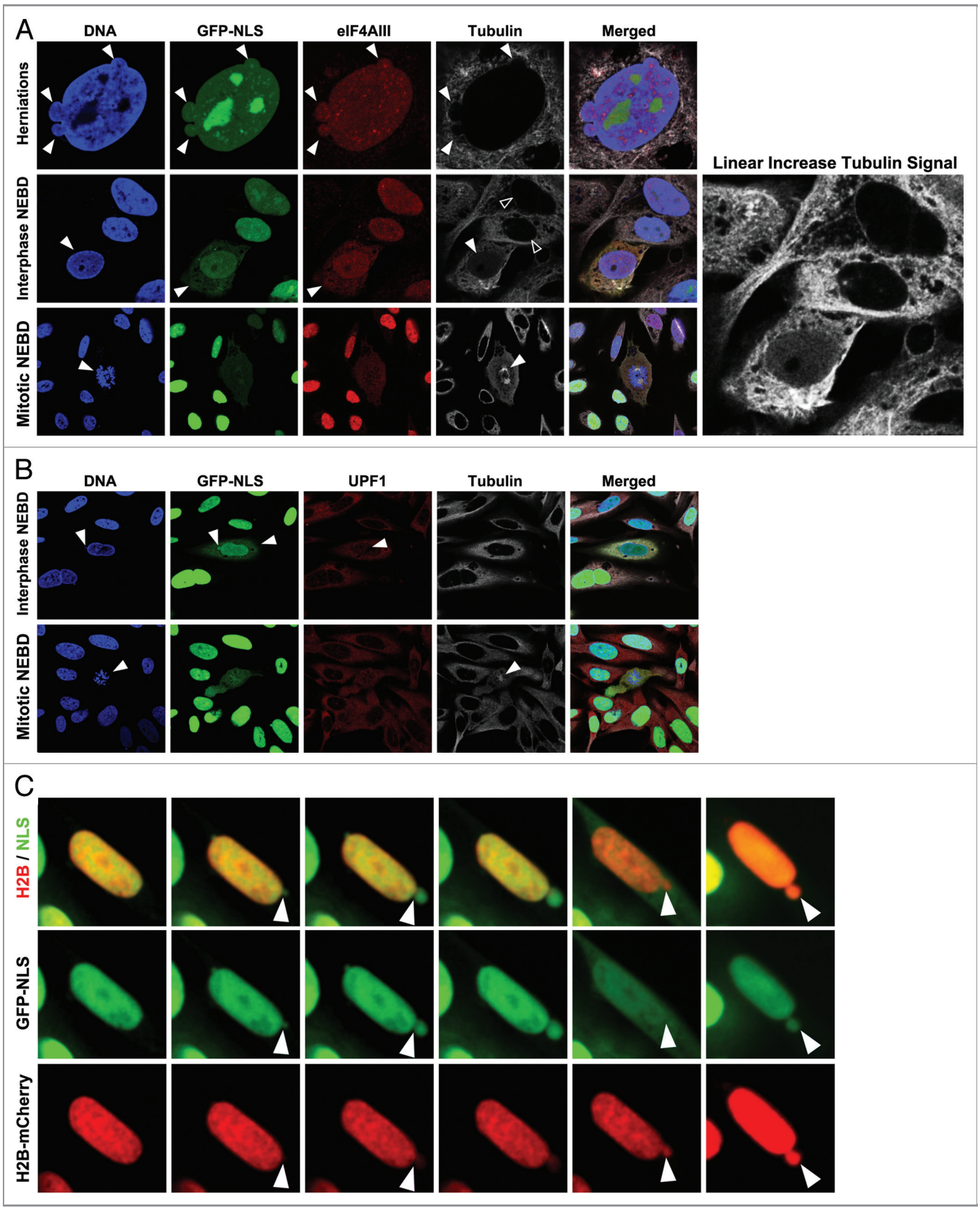
Figure 3. For figure legend, see page 93.

Since peripheral chromatin is in close proximity to the NE via interactions with the lamina and INM proteins,[43] we wondered whether NERDI, which likely results in the disruption of these interactions, could result in the loss of genomic material from the nucleus. To test this possibility, we expressed H2B-mCherry, which localizes exclusively to chromatin throughout the cell cycle,[18] and GFP$_3$-NLS in U2OS cells in which the three lamins had been depleted. Analysis of still images of an interphase NE rupture event clearly shows the presence of H2B-mCherry within NE deformations, as indicated by co-localization with GFP$_3$-NLS (**Fig. 3C**, left panels arrows). The presence of DNA in NE herniations is also supported by the observation of Hoechst labeling of these structures in immunofluorescent images of U2OS cells stably reduced for lamin B1 expression (see **Fig. 3A**). The NE deformation eventually ruptures, as indicated by the diffuse cytoplasmic GFP$_3$-NLS signal, and notably during this event H2B-mCherry also extends beyond the pre-rupture nuclear boundary, but with a more limited range (**Fig. 3C**, bottom panels arrows). The localization pattern of the H2B-mCherry signal is inconsistent with it being soluble and freely diffusible during the rupture (compare with GFP$_3$-NLS, **Fig. 3C** middle panels), and instead indicates that NERDI alters chromatin organization at the site of rupturing. After repair of the NE, indicated by nuclear accumulation of GFP$_3$-NLS, H2B-mCherry remains segregated within an extra-nuclear body (**Fig. 3C**, right panels arrows). Genomic instability is a hallmark of cancer and our data showing a persistent presence of chromatin outside the normal nuclear boundary make it plausible for premature rupturing of the NE to contribute to chromosome aberrations that accumulate over time in cancer cells. Our live-imaging results frequently show these extra-nuclear particles moving great distances from the post-rupture repaired NE (**Vid. S3**). If these particles contain genomic information, the potential for mutagenesis is virtually certain.

NE rupturing causes temporary loss of cellular compartmentalization. We next asked whether mislocalization of cytosolic components during NERDI is limited to soluble proteins by examining organelle localization during NERDI. We examined mitochondria localization by expressing pTurboRFP-mito in U2OS cells depleted of lamin B1 and expressing the integrity reporter GFP$_3$-NLS. We were able to clearly observe mitochondria present in the nucleus of cells, as indicated by 3D reconstruction (**Fig. 4A**, **Vid. S5**). In addition, cytoplasmic components within the nucleus were visible in knockdown cells by TEM (**Fig. 4B**, i and ii). These structures do not represent nuclear invaginations since they lack the double membrane with ribosome decoration that characterizes the NE (**Fig. 4B**, iii). Although we cannot exclude the possibility that some of these organelles are trapped during NE reformation after mitosis, it is unlikely that this is the case as nuclear envelope formation membrane recruitment to chromatin happens during a highly compacted chromatin state with ER membrane tubules being recruited to and flattening directly on the chromatin surface.[18,20] To that end, attempts to physically drag mitochondria into the nucleus during NEF by tagging mitochondrial membrane proteins with chromatin binding domains failed to cause nuclear

entrapment (data not shown). Our observations of mitochondria and other cytoplasmic organelles in cells with a high frequency of NERDI are consistent with results from a recent study of laminopathy cells that also found intranuclear mitochondria associated with interphase NE rupturing.[22] The movement of organelles into the nucleus could have severe consequences for the cell since structures of this size are likely to be trapped inside the nucleus for the duration of interphase.

Discussion

The NE partitions the eukaryotic cell into two compartments between which there is a highly regulated exchange of proteins, nucleic acids, and cellular activities. With the delineation of specific cellular processes to distinct and separate spaces, spatial regulation is able to add to the complex series of pathways that control normal cellular physiology. Nuclear-cytoplasmic transport, which occurs through the nuclear pore complex, is an important aspect of normal cell function, and defects in this process have been reported in human genetic diseases and in divergent types of cancer.[44] These defects can occur in the signal-transduction pathways that regulate the transfer of factors such as p53 and β-catenin in and out of the nucleus, or in the general nuclear import and export machinery itself.[44] Our results show that the most dramatic example of compromised spatial identity in the cell may well be NERDI. We describe a phenomenon in cancer cells where the interphase NE transiently ruptures, mixing nucleoplasm and cytoplasm. We show that decreased lamin expression leads to localized deformation of the NE that expands and eventually ruptures, leading to the mixing of nuclear and cytoplasmic components and transiently abrogating proper cellular compartmentalization (**Fig. 4C**). Consequences of this event include mislocalization of proteins, changes to the containment of the genome, and the introduction of large cytoplasmic structures into the protected nuclear space. The uncontrolled movement of macromolecules across a ruptured NE is likely to perturb processes dependent on compartmentalized localization of regulatory proteins such as cell growth pathways, potentially contributing to neoplastic transformation.

Furthermore, nuclear export of properly processed mRNAs is a critical component of eukaryotic gene expression. The complex life cycle of gene transcription products is performed initially in the nuclear interior and then shifted to cytoplasmic space for final translation. This movement of mRNA between cellular spaces is a target of regulation and our demonstration of the mislocalization of proteins involved in mRNA processing poses interesting questions for the study and interpretation of results from mRNA maturation studies. NE rupturing might lead to the efflux of entire mRNP complexes that are not properly spliced and processed, or in RNA processing factors loosing proper cellular compartmentalization, possibly resulting in aberrant translation products or degradation of the respective RNAs.

An important consideration in light of this work is the fact that countless studies over the last decades have used cancer cell lines to study the cell cycle, signal transduction pathways and DNA damage and repair. An underlying assumption of all these studies
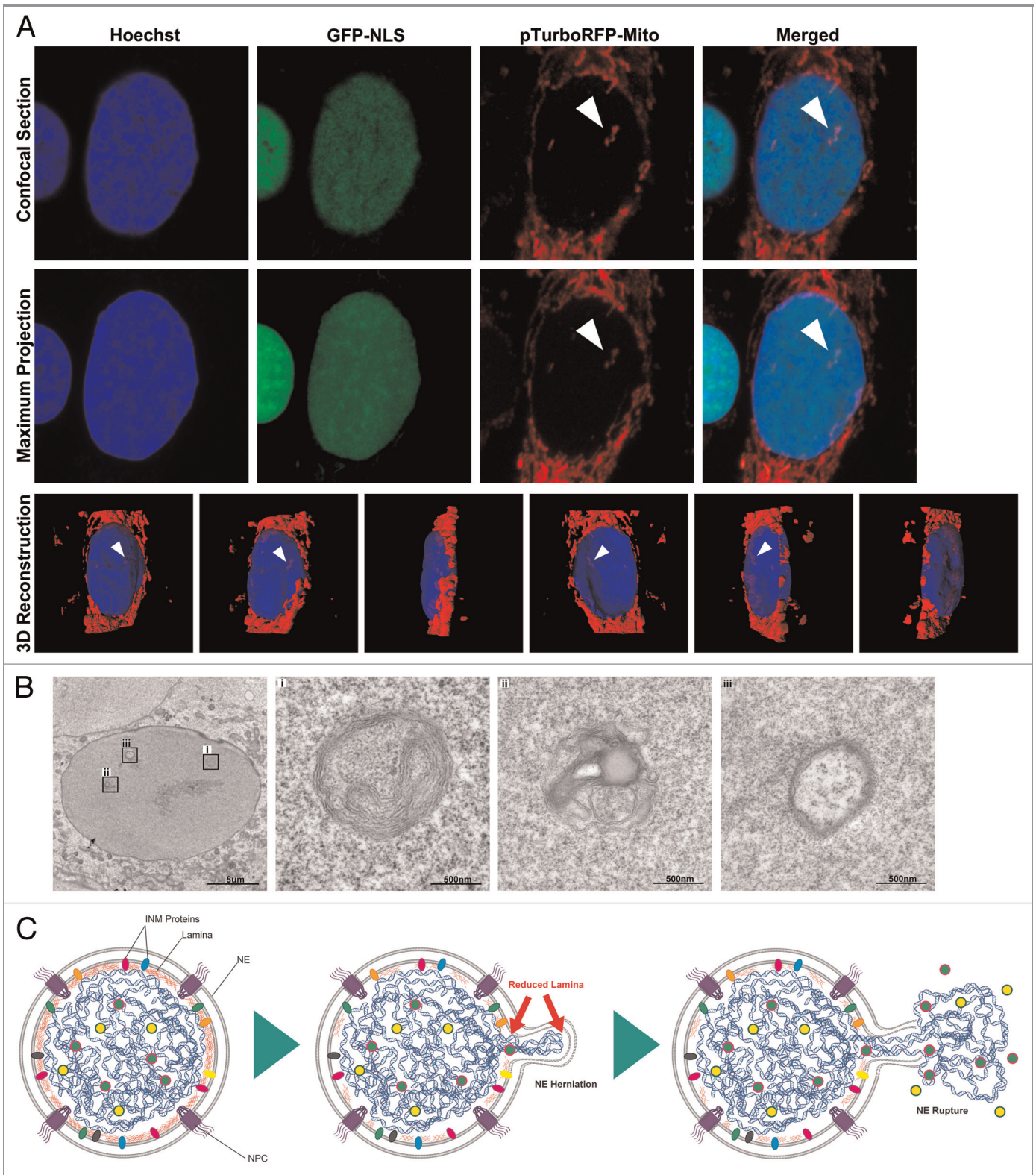
Figure 4. Consequences of interphase nuclear rupture. (A) U2OS cells expressing GFP₃-NLS (green) and pTurboRFP-mito (red), and stained for DNA with Hoechst (blue) show nuclear mitochondria in confocal slice (top), maximum intensity projection (middle) and 3D reconstruction with nuclear mitochondria indicated (arrows). (B) TEM of U2OS cells stably reduced for lamin B1 expression by shRNA showing cytoplasmic bodies enclosed within the nucleus (i and ii) contrasted from nuclear invaginations with characteristic NE double membrane and ribosome decoration (iii). (C) Proposed model for Nuclear Envelope Rupture During Interphase (NERDI) in cancer cells. Reduced lamin expression leads to a weakened NE that distends outward, eventually rupturing with a mixing of nuclear and cytoplasmic components.

was that the NE breaks down only during mitosis, when the majority of transcription is halted and when chromatin is in a highly compacted state. Realizing that, at least in some of the most frequently used cell lines, the NE transiently ruptures in a small subset of cells may lead to a new evaluation of previous results. Interphase NE rupturing suggests that additional levels of nuclear-cytoplasmic communications exist and may bring new insights to transcriptional regulation and gene expression studies or other work involving factors with regulated movement between the nuclear and cytoplasmic compartments.

In addition to its role in mediating signal-dependent, active nuclear transport, a long proposed cellular function for the evolution of the NE is to form a protective shield around the nuclear genome and thereby prevent the direct contact between cytoplasmic proteins, organelles, and metabolic by-products and the nuclear DNA. Our findings that organelles and cytoplasmic components can enter the interphase nucleus suggest that, in some cancer cells, eukaryotic cell organization is compromised and may result in insult to the genome. The presence of such components in the nucleus during interphase, when DNA is replicated and transcriptional programs are executed, could be a source of DNA damage that has not yet been appreciated. Cellular organelles such as mitochondria generate a high number of reactive oxygen species that, without the proper machinery present to neutralize them, could induce mutagenesis. Of note, the presence of cytoplasmic structures, including mitochondria, vacuoles and Golgi fragments inside the nuclei of neoplastic cells has been observed repeatedly by EM[45] without a concrete explanation or mechanism for their presence. Furthermore, 'nuclear mitochondria' were observed in lymphoid tumors over three decades ago,[46] suggesting that this phenomenon might be relevant for tumor formation in vivo. Our results provide a cell biological explanation for the presence of these 'nuclear cytoplasmic bodies.'

Why does NE rupturing in interphase occur in cancer cells but not, or very infrequently, in primary cells? One explanation could be that the mechanical properties of the NE in cancer cells are different from non-cancer cells. For instance, loss of lamin expression or altered lamin structure is often found in cancer cells, including leukemia and lymphoma,[47-49] colon cancer,[50] prostatic cancer,[51] gastric cancer[24] and lung cancer.[25,52] Our data, along with results from other labs and studies of the affect of lamin loss on nuclear elastic properties, indicate that low lamin levels or aberrant lamina organization might make the NE more susceptible to rupture. One striking feature of NE rupturing during interphase is that it is reversible, with cells able to recover and go on to produce progeny. Therefore, a mechanism must be in place to re-seal the double membrane, suggesting that the phenomenon has existed long enough for cells to have adapted a response. This is the first example of a NE repair mechanism outside of mitotic context and underscores the dynamic organization of the NE at a level that has not previously been appreciated.

The failure to properly localize nuclear components as a result of defective nuclear transport has been directly associated with defects in chromatin organization and gene regulation.[44] Since the NE is commonly thought to remain intact during interphase, all nucleo-cytoplasmic communication is thought to occur through NPCs. The discovery that the NE undergoes transient rupturing during interphase establishes a novel example of aberrant nucleo-cytoplasmic communication that does not depend on trafficking through NPCs. Unlike controlled nuclear-cytoplasmic transport, this loss of the NE barrier function likely represents a catastrophic event that potentially affects the regulation of multiple cellular processes, with apparent changes to the localization of parts of the genome in the extreme cases.

Micronucleation has long been considered to result from imperfect segregation of acentric chromosomal fragments or fragments of overly long chromosomes during karyokinesis.[53,54] A study has previously shown that acentric double minute chromosomes (DMs) can be sorted to the nuclear periphery during S phase and then selectively eliminated from the nucleus by micronucleation in advance of karyokinesis.[55] Our results provide evidence that fragmentation of the nuclear genome may occur in interphase associated with the phenomenon of NE rupturing.

Despite our substantial understanding of molecular mechanisms and gene mutations involved in cancer, the technical approaches for diagnosis and prognosis of cancer are still limited. A deformed and enlarged nuclear morphology is a common characteristic of cancer cells, and the "roundness" of the nucleus is a good indicator to distinguish benign, low grade, and malignant cells.[2] In the clinical setting, the morphology of the nucleus is used universally for diagnostic and prognostic prediction of malignancies of tumor cells, referred to as "nuclear grade."[2] Linking cytological information such as aberrant nuclear morphology with functional data (e.g., NE rupturing) could help develop new diagnostic tools or refine existing ones. Our results will increase our understanding of pathological NE organization and might open new avenues for clinical diagnostics.

Materials and Methods

Cell culture. U2OS, HeLa, SJSA and MCF7 cell lines were cultured according to standard tissue culture practices and maintained in the logarithmic phase of growth in DMEM (CellGo) supplemented with 10% fetal bovine serum (HyClone), penicillin, and streptomycin. IMR90 cell line was cultured in DMEM with Glutamax (Gibco) supplemented with 20% fetal bovine serum (HyClone) and non-essential amino acids (CellGo).

siRNA transfection. Cells were transfected twice at 2d and 4d prior to analysis using 0.6μl Lipofectamine 2000 (Invitrogen) with 25–50 nmol of the siRNA oligos: Lamin A/C (UGU UCU UCU GGA AGU CCA GTT), lamin B1 (CGC GCU UGG UAG AGG UGG ATT), lamin B2 (ACU CGG CUU CCU CCU CCU CTT), scrambled (UAG ACA CCA UGC ACA AUC CTT), LBR, Lap2b, Nup93, and Nup 107 (sequences previously reported in refs. 18 and 20).

Expression constructs. GFP$_3$-NLS was constructed using the Gateway system (Invitrogen) to insert a sequence of tandem EGFPs and the NLS (PPKKKRKV) from the SV40 large T antigen into the N-terminal cycle3-GFP containing vector, pcDNA6.2/DEST53. FLAG-Vpr was a generous gift of Warner Greene

(UCSF, San Francisco, CA USA,) H2B-mCherry and GFP-IBB were generous gifts of Michael Schmitz and Daniel Gerlich (ETH, Zurich, Switzerland). The mCherry-lamin B2 construct was made by inserting full-length lamin B2 (a gift from Harald Hermann, DKFZ, Heidelberg, Germany) into mCherry-DEST vector (a gift from Clodagh O'Shea, the Salk Institute, La Jolla CA, USA). Sec61b-GFP was previously reported. mCherry-tubulin was a generous gift from Chris Somerville (UC Berkeley, Berkeley CA, USA). pTurboRFP-Mito was purchased from Evrogen.

Stable cell lines. The lamin B1 shRNA stable cell line was generated by first transiently transfecting GFP$_3$-NLS into U2OS cells and selecting with G418 after 48 h. Cells were propagated for 2 weeks under G418 selection and then the GFP$^+$ population collected by FACS. The GFP+ population was then infected with lenti-viral particles carrying a pLKO.1 plasmid containing an shRNA directed against lamin B1 (OpenBiosystems) and selected after 48 h with puromycin. Cells were carried in both selective markers for 6 passages and stocks frozen. Cells were maintained in both selection markers for the duration of imaging experiments.

Immunofluorescence and protein gel blot antibodies. Primary antibodies used in this study are: rabbit α-eIF4AIII and rabbit α-UPF1 were kind gifts from Jens Lykke-Andersen, UC San Diego, La Jolla, CA USA, rabbit α-lamin A (Sigma), goat α-lamin B1 (Santa Cruz), mouse α-lamin B2 (Abcam), rabbit α-FLAG (Cell Signaling), and mouse α-tubulin (Sigma). Secondary antibodies are, from Invitrogen: goat α-mouse Alexa Fluor 488, goat α-rabbit Alex Fluor 488, donkey α-goat Alexa Fluor 488, goat α-mouse Alexa Fluor 568, goat α-rabbit Alexa Fluor 568, goat α-mouse Alexa Fluor 647, goat α-rabbit Alexa Fluor 647, and donkey α-goat Alexa Fluor 647; and from Li-Cor: goat α-mouse IRDye 680, goat α-rabbit IRDye 680, donkey α-goat IRDye 680, donkey α-mouse IRDye 800, and donkey α-rabbit IRDye 800.

Protein gel blotting and whole cell lysates. Whole cell lysates were collected at 70–90% confluency by washing twice in PBS, scraping in lysis buffer, and protein concentration normalized using BCA Protein Assay kit (Pierce). MDAMB, HCC and HMEC lysates were a generous gift from Clodagh O'Shea, the Salk Institute, La Jolla, CA, USA. Protein gel blotting was performed using the indicated primary and secondary antibodies. Blots were analyzed on the Li-Cor Odyssey system and processed using Photoshop CS5 extended (Adobe).

Live and confocal imaging. Live-imaging was performed in 8 well μ-slide chambers (iBidi) on either a Yokagawa spinning disk built around a Leica DMRIE2 inverted confocal microscope with a 20x air or 63x 1.4NA oil immersion objective at 37°C maintained by a CO$_2$ enriched air stream incubator (Solent Scientific) and images captured with an EM CCD (Hamamatsu) using SimplePCI software (Compix) or on a Zeiss/Yokagawa spinning disk inverted confocal microscope with a 20x air or 63x 1.4NA oil immersion objective at 37°C maintained by a CO$_2$ enriched air stream incubator (Pecon) and images captured with an EM CCD (Hamamatsu) using AxioVision software (Zeiss). For fixed imaging, cells were grown on glass coverslips and images were acquired on either a Leica SP2 scanning confocal microscope

with a 63x 1.4NA oil immersion objective with LCS software (Leica), or on a Zeiss LSM 710 scanning confocal microscope with a 63x 1.4NA oil immersion objective with Zen software (Zeiss). Fluorochromes and stains used in this study are EGFP, cycle3GFP, mCherry, Alexa Fluor 488, Alexa Fluor 568, Alexa Fluor 647, Hoechst 33342 (Molecular Probes), and MitoTracker Red CMX$_{ros}$ (Invitrogen).

Electron microscopy. Cells were grown in 35mm plastic culture dishes were fixed using the protocol of Gilula et al. (1978).[56] The cells were fixed in 2.5% glutaraldehyde in 0.1M Na cacodylate buffer (pH7.3), buffer washed and fixed in 1% osmium tetroxide in 0.1M Na cacodylate buffer. They were subsequently treated with 0.5% tannic acid followed by 1% sodium sulfate in cacodylate buffer and then dehydrated in graded ethanol series. The cells were cleared in HPMA (2-hydroxypropyl methacrylate: Ladd Research) and embedded in LX112 resin. Following overnight polymerization at 60°C, small pieces of resin were attached to blank blocks using SuperGlue (Scotch). Thin sections (70nm) were cut on a Reichert Ultracut E (Leica) using a diamond knife (Diatome, Electron Microscopy Sciences), mounted on parlodion coated, copper, slot grids and stained in uranyl acetate and lead citrate. Sections were examined at 80kV on a Philips CM100 TEM (FEI) and data documented on a Megaview III CCD camera (Olympus Soft Imaging Solutions).

Image processing and data analysis. Images were analyzed and processed for display using Photoshop CS5 extended (Adobe). Spilling frequency was determined using a MatLab (Mathworks) nuclei counting algorithm to count total number of cells, movies were then analyzed manually, frame by frame, for interphase nuclear ruptures. The number of times each cell ruptured was also tabulated and the average of this number used to determine the frequency of ruptures within individual cells. Statistics were performed using either Prism 5 (GraphPad) or Excel 2011 (Microsoft). Curve fitting of rupture dynamics was done using Prism 5 (GraphPad) as described in the text.

3D reconstruction. Optimized confocal z-series were acquired on a Zeiss LSM 710 scanning confocal microscope and assembled into 3D surfaces for each channel by absolute intensity and with thresholding adjusted so that generated surfaces are matched to fluorescence signal using Imaris (BitPlane).

References

1. Zink D, Fischer AH, Nickerson JA. Nuclear structure in cancer cells. Nat Rev Cancer 2004; 4:677-87; PMID:15343274; http://dx.doi.org/10.1038/nrc1430

2. Fischer AH, Zhao C, Li QK, Gustafson KS, Eltoum IE, Tambouret R, et al. The cytologic criteria of malignancy. J Cell Biochem 2010; 110:795-811; PMID:20564180; http://dx.doi.org/10.1002/jcb.22585

3. Hannen EJ, van der Laak JA, Manni JJ, Pahlplatz MM, Freihofer HP, Slootweg PJ, et al. An image analysis study on nuclear morphology in metastasized and non-metastasized squamous cell carcinomas of the tongue. J Pathol 1998; 185:175-83; PMID:9713344; http://dx.doi.org/10.1002/(SICI)1096-9896(199806)185:2<175::AID-PATH69>3.0.CO;2-U

4. Broers JL, Peeters EA, Kuijpers HJ, Endert J, Bouten CV, Oomens CW, et al. Decreased mechanical stiffness in LMNA−/− cells is caused by defective nucleo-cytoskeletal integrity: implications for the development of laminopathies. Hum Mol Genet 2004; 13:2567-80; PMID:15367494; http://dx.doi.org/10.1093/hmg/ddh295

5. Lammerding J, Schulze PC, Takahashi T, Kozlov S, Sullivan T, Kamm RD, et al. Lamin A/C deficiency causes defective nuclear mechanics and mechanotransduction. J Clin Invest 2004; 113:370-8; PMID:14755334

6. Newport JW, Wilson KL, Dunphy WG. A lamin-independent pathway for nuclear envelope assembly. J Cell Biol 1990; 111:2247-59; PMID:2277059; http://dx.doi.org/10.1083/jcb.111.6.2247

7. Lammerding J, Fong LG, Ji JY, Reue K, Stewart CL, Young SG, et al. Lamins A and C but not lamin B1 regulate nuclear mechanics. J Biol Chem 2006; 281:25768-80; PMID:16825190; http://dx.doi.org/10.1074/jbc.M513511200

8. Dittmer TA, Misteli T. The lamin protein family. Genome Biol 2011; 12:222; PMID:21639948; http://dx.doi.org/10.1186/gb-2011-12-5-222

9. Vergnes L, Peterfy M, Bergo MO, Young SG, Reue K. Lamin B1 is required for mouse development and nuclear integrity. Proc Natl Acad Sci USA 2004; 101:10428-33; PMID:15232008; http://dx.doi.org/10.1073/pnas.0401424101

10. Worman HJ, Ostlund C, Wang Y. Diseases of the nuclear envelope. Cold Spring Harb Perspect Biol 2010; 2:a000760; PMID:20182615; http://dx.doi.org/10.1101/cshperspect.a000760

11. Sullivan T, Escalante-Alcalde D, Bhatt H, Anver M, Bhat N, Nagashima K, et al. Loss of A-type lamin expression compromises nuclear envelope integrity leading to muscular dystrophy. J Cell Biol 1999; 147:913-20; PMID:10579712; http://dx.doi.org/10.1083/jcb.147.5.913

12. Lee JS, Hale CM, Panorchan P, Khatau SB, George JP, Tseng Y, et al. Nuclear lamin A/C deficiency induces defects in cell mechanics, polarization, and migration. Biophys J 2007; 93:2542-52; PMID:17631533; http://dx.doi.org/10.1529/biophysj.106.102426

13. Raharjo WH, Enarson P, Sullivan T, Stewart CL, Burke B. Nuclear envelope defects associated with LMNA mutations cause dilated cardiomyopathy and Emery-Dreifuss muscular dystrophy. J Cell Sci 2001; 114:4447-57; PMID:11792810

14. Burke B, Stewart CL. The laminopathies: the functional architecture of the nucleus and its contribution to disease. Annu Rev Genomics Hum Genet 2006; 7:369-405; PMID:16824021; http://dx.doi.org/10.1146/annurev.genom.7.080505.115732

15. Margalit A, Vlcek S, Gruenbaum Y, Foisner R. Breaking and making of the nuclear envelope. J Cell Biochem 2005; 95:454-65; PMID:15832341; http://dx.doi.org/10.1002/jcb.20433

16. Foisner R. Cell cycle dynamics of the nuclear envelope. ScientificWorldJournal 2003; 3:1-20; PMID:12806116; http://dx.doi.org/10.1100/tsw.2003.06

17. Hetzer MW. The nuclear envelope. Cold Spring Harb Perspect Biol 2010; 2:a000539; PMID:20300205; http://dx.doi.org/10.1101/cshperspect.a000539

18. Anderson DJ, Vargas JD, Hsiao JP, Hetzer MW. Recruitment of functionally distinct membrane proteins to chromatin mediates nuclear envelope formation in vivo. J Cell Biol 2009; 186:183-91; PMID:19620630; http://dx.doi.org/10.1083/jcb.200901106

19. Gerace L, Foisner R. Integral membrane proteins and dynamic organization of the nuclear envelope. Trends Cell Biol 1994; 4:127-31; PMID:14731735; http://dx.doi.org/10.1016/0962-8924(94)90067-1

20. Anderson DJ, Hetzer MW. Reshaping of the endoplasmic reticulum limits the rate for nuclear envelope formation. J Cell Biol 2008; 182:911-24; PMID:18779370; http://dx.doi.org/10.1083/jcb.200805140

21. Anderson DJ, Hetzer MW. Shaping the endoplasmic reticulum into the nuclear envelope. J Cell Sci 2008; 121:137-42; PMID:18187447; http://dx.doi.org/10.1242/jcs.005777

22. De Vos WH, Houben F, Kamps M, Malhas A, Verheyen F, Cox J, et al. Repetitive disruptions of the nuclear envelope invoke temporary loss of cellular compartmentalization in laminopathies. Hum Mol Genet 2011; 20:4175-86; PMID:21831885; http://dx.doi.org/10.1093/hmg/ddr344

23. Venables RS, McLean S, Luny D, Moteleb E, Morley S, Quinlan RA, et al. Expression of individual lamins in basal cell carcinomas of the skin. Br J Cancer 2001; 84:512-9; PMID:11207047; http://dx.doi.org/10.1054/bjoc.2000.1632

24. Moss SF, Krivosheyev V, de Souza A, Chin K, Gaetz HP, Chaudhary N, et al. Decreased and aberrant nuclear lamin expression in gastrointestinal tract neoplasms. Gut 1999; 45:723-9; PMID:10517909; http://dx.doi.org/10.1136/gut.45.5.723

25. Broers JL, Raymond Y, Rot MK, Kuijpers H, Wagenaar SS, Ramaekers FC. Nuclear A-type lamins are differentially expressed in human lung cancer subtypes. Am J Pathol 1993; 143:211-20; PMID:8391215

26. Machiels BM, Broers JL, Raymond Y, de Ley L, Kuijpers HJ, Caberg NE, et al. Abnormal A-type lamin organization in a human lung carcinoma cell line. Eur J Cell Biol 1995; 67:328-35; PMID:8521872

27. Jansen MP, Machiels BM, Hopman AH, Broers JL, Bot FJ, Arends JW, et al. Comparison of A and B-type lamin expression in reactive lymph nodes and nodular sclerosing Hodgkin's disease. Histopathology 1997; 31:304-12; PMID:9363444; http://dx.doi.org/10.1046/j.1365-2559.1997.2820881.x

28. Marmé A, Zimmermann HP, Moldenhauer G, Schorpp-Kistner M, Muller C, Keberlein O, et al. Loss of Drop1 expression already at early tumor stages in a wide range of human carcinomas. Int J Cancer 2008; 123:2048-56; PMID:18709643; http://dx.doi.org/10.1002/ijc.23763

29. Kaufmann SH. Expression of nuclear envelope lamins A and C in human myeloid leukemias. Cancer Res 1992; 52:2847-53; PMID:1581898

30. Kaufmann SH, Mabry M, Jasti R, Shaper JH. Differential expression of nuclear envelope lamins A and C in human lung cancer cell lines. Cancer Res 1991; 51:581-6; PMID:1985776

31. Capo-chichi CD, Cai KQ, Simpkins F, Ganjei-Azar P, Godwin AK, Xu XX. Nuclear envelope structural defects cause chromosomal numerical instability and aneuploidy in ovarian cancer. BMC Med 2011; 9:28; PMID:21439080; http://dx.doi.org/10.1186/1741-7015-9-28

32. Capo-chichi CD, Cai KQ, Smedberg J, Ganjei-Azar P, Godwin AK, Xu XX. Loss of A-type lamin expression compromises nuclear envelope integrity in breast cancer. Chin J Cancer 2011; 30:415-25; PMID:21627864; http://dx.doi.org/10.5732/cjc.010.10566

33. Haraguchi T, Koujin T, Hayakawa T, Kaneda T, Tsutsumi C, Imamoto N, et al. Live fluorescence imaging reveals early recruitment of emerin, LBR, RanBP2, and Nup153 to reforming functional nuclear envelopes. J Cell Sci 2000; 113:779-94; PMID:10671368

34. de Noronha CM, Sherman MP, Lin HW, Cavrois MV, Moir RD, Goldman RD, et al. Dynamic disruptions in nuclear envelope architecture and integrity induced by HIV-1 Vpr. Science 2001; 294:1105-8; PMID:11691994; http://dx.doi.org/10.1126/science.1063957

35. Dahl KN, Scaffidi P, Islam MF, Yodh AG, Wilson KL, Misteli T. Distinct structural and mechanical properties of the nuclear lamina in Hutchinson-Gilford progeria syndrome. Proc Natl Acad Sci USA 2006; 103:10271-6; PMID:16801550; http://dx.doi.org/10.1073/pnas.0601058103

36. De Vos WH, Houben F, Hoebe RA, Hennekam R, van Engelen B, Manders EM, et al. Increased plasticity of the nuclear envelope and hypermobility of telomeres due to the loss of A-type lamins. Biochim Biophys Acta 2010; 1800:448-58; PMID:20079404; http://dx.doi.org/10.1016/j.bbagen.2010.01.002

37. Dechat T, Pfleghaar K, Sengupta K, Shimi T, Shumaker DK, Solimando L, et al. Nuclear lamins: major factors in the structural organization and function of the nucleus and chromatin. Genes Dev 2008; 22:832-53; PMID:18381888; http://dx.doi.org/10.1101/gad.1652708

38. Stewart CL, Roux KJ, Burke B. Blurring the boundary: the nuclear envelope extends its reach. Science 2007; 318:1408-12; PMID:18048680; http://dx.doi.org/10.1126/science.1142034

39. Shimi T, Pfleghaar K, Kojima S, Pack CG, Solovei I, Goldman AE, et al. The A- and B-type nuclear lamin networks: microdomains involved in chromatin organization and transcription. Genes Dev 2008; 22:3409-21; PMID:19141474; http://dx.doi.org/10.1101/gad.1735208

40. Coffinier C, Chang SY, Nobumori C, Tu Y, Farber EA, Toth JI, et al. Abnormal development of the cerebral cortex and cerebellum in the setting of lamin B2 deficiency. Proc Natl Acad Sci USA 2010; 107:5076-81; PMID:20145110; http://dx.doi.org/10.1073/pnas.0908790107

41. Le Hir H, Andersen GR. Structural insights into the exon junction complex. Curr Opin Struct Biol 2008; 18:112-9; PMID:18164611; http://dx.doi.org/10.1016/j.sbi.2007.11.002

42. Chang YF, Imam JS, Wilkinson MF. The nonsense-mediated decay RNA surveillance pathway. Annu Rev Biochem 2007; 76:51-74; PMID:17352659; http://dx.doi.org/10.1146/annurev.biochem.76.050106.093909

43. Foisner R, Gerace L. Integral membrane proteins of the nuclear envelope interact with lamins and chromosomes, and binding is modulated by mitotic phosphorylation. Cell 1993; 73:1267-79; PMID:8324822; http://dx.doi.org/10.1016/0092-8674(93)90355-T

44. Kau TR, Way JC, Silver PA. Nuclear transport and cancer: from mechanism to intervention. Nat Rev Cancer 2004; 4:106-17; PMID:14732865; http://dx.doi.org/10.1038/nrc1274

45. Bernhard W, Granboulan N. The Fine Structure of the Cancer Cell Nucleus. Exp Cell Res 1963; 24(SUPPL9):L9-53; PMID:14046228

46. Brandes D, Schofield BH, Anton E. Nuclear mitochondria?. Science 1965; 149:1373-4; PMID:5889956; http://dx.doi.org/10.1126/science.149.3690.1373

47. Müller PR, Meier R, Hirt A, Bodmer JJ, Janic D, Leibundgut K, et al. Nuclear lamin expression reveals a surprisingly high growth fraction in childhood acute lymphoblastic leukemia cells. Leukemia 1994; 8:940-5; PMID:8207988

48. Collard JF, Senecal JL, Raymond Y. Redistribution of nuclear lamin A is an early event associated with differentiation of human promyelocytic leukemia HL-60 cells. J Cell Sci 1992; 101:657-70; PMID:1522148

49. Stadelmann B, Khandjian E, Hirt A, Luthy A, Weil R, Wagner HP. Repression of nuclear lamin A and C gene expression in human acute lymphoblastic leukemia and non-Hodgkin's lymphoma cells. Leuk Res 1990; 14:815-21; PMID:2232854; http://dx.doi.org/10.1016/0145-2126(90)90076-L

50. Belt EJ, Fijneman RJ, van den Berg EG, Bril H, Delis-van Diemen PM, Tijssen M, et al. Loss of lamin A/C expression in stage II and III colon cancer is associated with disease recurrence. Eur J Cancer 2011; 47:1837-45; PMID:21621406; http://dx.doi.org/10.1016/j.ejca.2011.04.025

51. Skvortsov S, Schafer G, Stasyk T, Fuchsberger C, Bonn GK, Bartsch G, et al. Proteomics profiling of micro-dissected low- and high-grade prostate tumors identifies Lamin A as a discriminatory biomarker. J Proteome Res 2011; 10:259-68; PMID:20977276; http://dx.doi.org/10.1021/pr100921j

52. Kaufmann SH, Mabry M, Jasti R, Shaper JH. Differential expression of nuclear envelope lamins A and C in human lung cancer cell lines. Cancer Res 1991; 51:581-6; PMID:1985776

53. Heddle JA, Carrano AV. The DNA content of micro-nuclei induced in mouse bone marrow by gamma-irradiation: evidence that micronuclei arise from acentric chromosomal fragments. Mutat Res 1977; 44:63-9; PMID:331097; http://dx.doi.org/10.1016/0027-5107(77)90115-4

54. Heddle JA, Hite M, Kirkhart B, Mavournin K, MacGregor JT, Newell GW, et al. The induction of micronuclei as a measure of genotoxicity. A report of the U.S. Environmental Protection Agency Gene-Tox Program. Mutat Res 1983; 123:61-118; PMID:6888413

55. Shimizu N, Kanda T, Wahl GM. Selective capture of acentric fragments by micronuclei provides a rapid method for purifying extrachromosomally amplified DNA. Nat Genet 1996; 12:65-71; PMID:8528254; http://dx.doi.org/10.1038/ng0196-65

56. Gilula NB, Epstein ML, Beers WH. Cell-to-cell communication and ovulation. A study of the cumulus-oocyte complex. J Cell Biol 1978; 78:58-75; PMID:670298; http://dx.doi.org/10.1083/jcb.78.1.58